Pressure and Temperature Dependence of the Hydrogen Bonding in Supercritical Ethanol: A Computer Simulation Study

Dimitris Dellis, Michalis Chalaris, and Jannis Samios*

Laboratory of Physical Chemistry, Department of Chemistry, University of Athens, Panepistimiopolis, Athens 157-71, Greece

Received: April 3, 2005; In Final Form: July 11, 2005

As a step toward deeper insight on the "hydrogen bonding" in supercritical ethanol (scEtOH), we carried out NVT molecular dynamics simulations of the fluid over a wide range of temperatures and pressures. The fluid was studied at SC conditions for which thermodynamic and spectroscopic (NMR, infrared, Raman, dielectric) data are available. The various site−site pair distribution functions (pdf's) were calculated, and their temperature and pressure dependence was obtained. It was found that over the thermodynamic conditions investigated here, scEtOH remains highly structured. Moreover, the characteristic behavior of the first peaks in H−H, O−O, and H−O pdf's reveals that hydrogen bonds still exist in scEtOH. The analysis focuses also on the reorientational dynamics of the bond unit vectors O−H, C−O, and of the permanent dipole moment of the molecules as well as the total dipole moment of the sample. The corresponding Legendre time correlation functions were discussed in connection to the "hydrogen bonding" in the fluid and in the context of experimental results. Specifically, the behavior of the O−H dynamics exhibits the well-known associative nature of the molecules in the system. A further analysis of the hydrogen bonds was carried out, and the degree of aggregation (average number of H-bonds per molecule) was obtained and compared with results from NMR chemical shift studies. Also the estimated monomer and free O−H groups in the fluid were compared with results from IR and Raman vibrational spectroscopy. The percentage analysis f_i of the liquid and scEtOH molecules, with $i = 0, 1, 2, 3, ...$ hydrogen bonds per molecule, has been obtained. The results show the existence of small, linear-chain oligomers formed mainly by two molecules, whereas the number of the three body oligomers, and specifically that of four body oligomers in the sample, is relatively small.

1. Introduction

During the past several decades, the properties of self-associated liquids assigned to hydrogen bonding (hereafter abbreviated as H-bonding), such as pure water, alcohols, and aqueous solutions, have been extensively studied.[1−3] Numerous studies concerning thermodynamic measurements, X-ray and neutron diffraction (ND), IR, Raman, and NMR spectroscopy, dielectric relaxation, etc., have been carried out in order to obtain information on the relationship between the degree of H-bonding and the physicochemical properties of the aforementioned systems.[4,5] Generally, due to the great importance of the H-bonds in many chemical and biological processes, experimental investigations aimed at the analysis of the H-bond network in associated liquids are a well-established and rapidly evolved research area.[6,7] A large number of recent publications and monographs illustrate the impressive progress that has been achieved in this research field since the introduction of some structurally and time-resolved sensitive new spectroscopic techniques used to study H-bonding in liquids.[8−12] For details, the reader is also referred to recent elegant reviews.[13,14] It should be mentioned, however, that despite the remarkable spectroscopic advances in a number of associated liquids so far, their H-bonding network and dynamics are poorly understood and fundamental questions on responsible molecular mechanisms remain. These mechanisms are important because they determine the way H-bonds are formed and broken.

From the theoretical point of view, the considerable importance of using pure theoretical techniques for predicting the structural and dynamic properties of H-bonded systems in condensed phase is obvious. However, since rigorous analytical and statistical mechanical theories cannot be easily developed especially in the case of self-associated materials, theoretical studies that aim at evaluating the degree of intermolecular H-bonding in such systems are usually based on atomistic computer simulations (CS).[15−29] Previous studies devoted to the properties of some of the most common self-associated liquids have shown that molecular dynamics simulations (MD) provide valuable information concerning the H-bonding network and dynamics in such systems.

Self-associated H-bonded fluids at supercritical conditions (SC) are well recognized as particularly important chemical intermediates in a number of fields of chemical technology. Thus, it is of considerable interest to investigate the properties of these systems at different SC conditions. In particular, a thorough investigation of the H-bonding network in such fluids is of foremost interest since H-bonding interactions play a crucial role in determining their physicochemical properties. Generally, supercritical fluids (SCFs) have found numerous applications in a number of chemical processes to date.[30] The use of many SCFs primarily as solvents is a consequence of their unique properties (adjustable solvating power and dielectric permittivity, low surface tension and viscosity, high diffusivity, etc.).[31] Therefore, knowledge about the thermophysical, structural, and dynamical properties of self-associated fluids at SC conditions

* To whom correspondence should be addressed. E-mail: isamios@cc.uoa.gr.

10.1021/jp051688a CCC: $30.25
Published on Web 09/10/2005

is essential for the sophisticated use of such systems and for further development of industrial applications.[32]

In recent years, there has been an increasing interest in experimental and theoretical studies of water particularly at near-critical (NC) and SC conditions for a number of reasons. Note, for instance, that SC water (SCW) is often used as a solvent in a variety of chemical reactions due to the characteristic behavior of its dielectric constant, the value of which can be continuously varied by adjusting the pressure.[33] More recently, the studies on SCW have been specifically devoted to the problem of H-bonding aimed at providing quantitative knowledge on the relationship between the properties of the fluid and the time-dependent changes in H-bonds geometry with temperature and/or pressure.[21−23,34−37]

Besides the motivation to learn more precisely about H-bonding in liquid and SCW as well as in aqueous mixtures, investigating the problem of aggregation in alcohols is of equal interest for many reasons. SC alcohols, for instance, may be used as alternative solvents[38] to water since these fluids possess an adjustable solvating power attributed to their relatively high dielectric constants and, furthermore, due to the fact that the thermodynamic conditions at their critical point are sufficiently lower than those of water. We mention also that among many polar organic compounds used widely as cosolvents with CO_2 at SC conditions ($scCO_2$) are mainly methanol (MeOH), ethanol (EtOH), and 2-propanol.[39] It is well-known that such SC mixed solvents can lead to an enhancement of the solubility of high molecular weight organic compounds in $scCO_2$.

Whereas much is known about the thermodynamic properties of pure alcohols and aqueous alcohol solutions, the quantitative determination of the local intermolecular structure and dynamics remains still quite challenging for most of these systems at SC conditions. Following the literature, we can notice that recent advances in spectroscopic techniques for studying H-bonded systems have widened the scientific interest in lower molecular weight SC alcohols. Nevertheless, there exist only a few spectroscopic studies on the structure and dynamics of pure SC alcohols reported so far. Specifically, we mention the NMR[40−44] and neutron diffraction (ND)[45] studies carried out by different groups. In addition, we found in the literature a number of spectroscopic studies devoted to these fluids using IR, Raman, UV−vis, and dielectric relaxation (DR) techniques.[46−51] The main goal in all these previous investigations has been the evaluation of the degree of H-bonding in the fluids under investigation in a wide temperature and pressure range. On the other hand, theoretical studies[52] and specifically atomistic CS studies on SC neat alcohols and their mixtures are scarce. To the best of our knowledge, there exist only a few MD studies devoted to the properties of scMeOH. Concretely, in two recent MD treatments,[53,54] we reported results concerning the H-bonding structure and dynamics of the liquid and scMeOH. The average number of H-bonds per molecule was obtained and compared with corresponding available results from NMR chemical shift measurements carried out by Hoffmann and Conradi.[40] The agreement between simulation and experiment was found to be quite good. In addition, we have been able to obtain a more quantitative picture[53] of the H-bonding network by determining the percentage distribution of H-bonds per molecule in liquid and scMeOH. Another study is that of Asahi and Nakamura,[42] who reported MD results on scMeOH performed in the same temperature and density range as their NMR chemical shift measurements. They also observed self-diffusion coefficients, which are found to be in good agreement with kinetic analytical theory and with results from MD simulation. Their MD simulations show that H-bonded clusters of methanol are chainlike both at room temperature and at SC conditions. Honma et al.[55] carried out a MD study of scMeOH using a flexible molecule potential model. The simulation of the fluid revealed a chainlike intermolecular structure in the liquid state and perturbed structure at SC conditions. They have also concluded that roughly half of the H-bonding molecules in the liquid state are preserved even at SC conditions. More recently, we reported results from MD simulations on SC mixtures of MeOH in CO_2[56] with MeOH mole fractions in the range of 0.0939−0.1173 at 323.15 K and pressure from 9.952 to 16.96 MPa. It is found that the structural and H-bonding results obtained reveal the existence of MeOH-type aggregates in the mixed fluid. This result was found to be in agreement with conclusions from previous experimental studies on this system. Finally, Yamaguchi et al.[44] carried out NMR experiments to study the single-molecule reorientational relaxation of SC methanol-d_4 and ethanol-d_6. They have also performed MD simulation of SC methanol-d_4 at the same conditions, and the results obtained are found to be consistent with those of the experiment.

The present work focuses on the properties of scEtOH by means of a series of extensive NVT-MD simulations. It is worth emphasizing that up to this point all previous CS studies of EtOH were restricted to the evaluation of the system properties at liquid conditions.[15,25,57−59] Note for instance that Guardia et al.[25] reported MD results on the influence of H-bonding upon different dynamic properties of liquid EtOH and other alcohols.

This study may be regarded as an extension of our previous MD simulations on scMeOH,[53,54] motivated by the newly appeared literature of spectroscopic works on scEtOH. Note that, as in the case of scMeOH, Hoffmann and Conradi[40] studied the degree of H-bonding in scEtOH up to 450 °C and over a wide range of pressures up to 350 bar. Hiejima and Yao[50] employed the dielectric relaxation method to study EtOH and 1-propanol in a wide fluid phase including the SC conditions. Finally, Besnard and co-workers[51] published a systematic vibrational experimental study on scEtOH that aimed at providing detailed information on the state of aggregation of pure scEtOH.

Our main objective here is to investigate the temperature and pressure dependence of the H-bonded structure of scEtOH and to give a more quantitative picture of the state of aggregation in the fluid. Finally, the paper is organized as follows: In subsection 2.1, we briefly review previously reported results on the state of H-bonding in scEtOH obtained experimentally. Subsection 2.2 is devoted to the description of the methodology and definitions employed to search and identify H-bonding structure during the simulation of the fluid. Details of the MD simulations are provided in subsection 2.3. Section 3 is devoted to the results concerning structural and dynamic properties of the system. The H-bonding analysis and statistics are presented in subsection 3.3. The main results and conclusions are summarized in section 4, while comparison between simulation and experimental data is presented throughout the paper.

2. Fundamentals

2.1. Evidence of H-Bonding in scEtOH. It is well-known from the literature that experimental studies are rather indirect methods to investigate the H-bonding local structure and dynamics in self-associated fluids. The main reason for this is the extremely short time scales of the relevant to the H-bonding network local elementary processes and intramolecular motions occurring in the ultrafast time domain from about 10 fs to several

picoseconds, which introduce substantial difficulties in the experimental studies. Note, for instance, that the well-known experimental diffraction techniques (X-ray, ND) provide time-averaged data of the local intermolecular structure. On the other hand, the most often employed dynamical spectroscopic and relaxation methods in studies of condensed molecular systems are not sufficiently sensitive to the time-dependent structural changes of the groups on the species participating in H-bonds. Thus, experimental methods that are structurally very sensitive (allowing for a separation of time scales on which microscopic dynamics occur) to the time-dependent changes in H-bonding local structure are the most suitable techniques to study H-bonds. Note, for instance, that combination of frequency and time domain spectroscopies in the time domain from a few femtoseconds to picoseconds have the potential to separate microscopic processes.

A rapidly evolving experimental technique in this direction that can be directly contacted to CS studies is the time-resolved IR vibrational spectroscopy. We mention here that time-resolved IR studies on liquid water have been recently reported and reviewed.[12−14] To the best of our knowledge, however, such experimental studies devoted to the H-bonding structure and dynamics of pure liquid and SC alcohols have not been reported so far.

As mentioned in the Introduction, spectroscopic studies based on standard techniques have been carried out for scEtOH, the outcome of which reveals the existence of H-bonding in the system. Concretely, in previous NMR studies[40−42] of scMeOH and scEtOH the authors pointed out that hydrogen bonds still exist in the fluids even at high temperatures and at very low gaslike densities. Specifically, the degree of H-bonding in scMeOH and scEtOH was found to be approximately 30% of that obtained in liquid MeOH and EtOH at 293 K. In addition, the authors in ref 42 pointed out that H-bonded clusters of alcohol molecules are chainlike both at room temperature and in the SC domain. Also, the number of H-bonded clusters decreases with increasing temperature and decreasing density. Note that the H-bonding formation energy and entropy were obtained from the temperature dependence of the OH chemical shifts for SC alcohols. The thermodynamic model, which takes account of cluster distribution, provides the degree of H-bonding in alcohols. Further to the experimental investigation of H-bonds in scEtOH, Besnard and co-workers[51] reported a study of the fluid combining IR absorption and Raman scattering vibrational spectroscopies. Their study was based on the OH stretching vibration mode of the EtOH molecule as a very sensitive group on the molecule participating in H-bonding. They have performed measurements at a temperature of 523 K and for densities in the range 0.01−0.6 g cm^{-3}. In that study the authors reported their results based on a quantitative band shape analysis supported by ab initio calculations carried out on small EtOH oligomers, namely, monomer, dimer, and cyclic as well as linear trimers. It is found that H-bonds still exist in scEtOH, a conclusion that is in agreement with those from previous studies and with ours from this study. In addition, these authors were able to estimate the percentage of free and H-bonded molecules as well as that of monomers, dimers, and trimers in the fluid at these SC conditions. They also found that the degree of H-bonding remains relatively constant above the critical density and becomes progressively broken below it.

In summary, the main conclusion that may be drawn from all the aforementioned spectroscopic investigations of scEtOH is that the large H-bonded aggregates observed in liquid EtOH clearly appear to be strongly reduced to small oligomers at SC conditions. Finally, a noticeable dependence of the degree of H-bonding in the fluid with pressure and temperature or density is strongly suggested by these experiments, and according to the results obtained from the present study it is clearly seen that the MD simulation technique can provide a detailed picture of the microscopical H− bonding structure of the fluid at these conditions.

2.2. H-Bonded Nearest-Molecules-Search Methodology. 2.2.1. Pair Distribution Functions. As a first step toward deeper insight into the details of the H-bonding structure of scEtOH, the various site−site pair distribution functions (pdf's), $g_{ij}(r)$, of the fluid were calculated and analyzed in the framework of this study. Each $g_{ij}(r)$ function is easily obtained from the trajectories of the molecules during the MD simulations by creating a corresponding histogram of the distances r_{ij}, calculating the average number density of molecules j identified in each spherical shell around the location of the central site, and finally dividing the resulting number density by the corresponding ensemble average one. The sites i and j are chosen to represent the center of mass (com) or a specific atom or group on different molecules. So, the pdf's were obtained for com−com, H−H, O−H, O−O, and Me−H. In the case of the com−com pdf's, the flexible character of the EtOH molecules introduced in the simulation has been taken into account by using the actual com of the molecules from one configuration to another. Additionally, to compare the structural directing effects of the different thermodynamic states, these pdf's were also calculated for the liquid EtOH at 298 K and normal pressure. All these functions have been constructed for distances up to about 14 Å with a resolution of 0.01 Å for all states of interest. These functions provide an accurate description of the short-range local order in dense fluids, which allows us to estimate the size of molecular aggregates by integrating over the first amplitude according to the well-known relation

$$\langle n_i \rangle = 1 + 4\pi\langle\rho\rangle \int_0^{r_c} g_{ij}(r) r^2 \, dr \qquad (1)$$

where $\langle\rho\rangle$ denotes the average number density. By choosing the upper integration limit, r_{min}, as the position of the first minimum in $g_{ij}(r)$, $\langle n_i \rangle$ reveals the number of species participating in the formation of a possible aggregate. In subsection 3.1, we report the simulated pdf's and we discuss them in connection to the H-bonding structure in the fluid.

2.2.2. H-Bonding Search Method. As mentioned in the Introduction, our target in this treatment is the investigation of the degree of H-bonding in scEtOH. Following the results of pdf's obtained in our previous studies on scMeOH, we may also expect a similar behavior of these functions for scEtOH. Concretely, from the calculated pdf's, and specifically from the first solvation shells in the case of the site−site H−O, H−H, and O−O functions, we expect a pronounced local order revealed by the presence of the first sharp peaks on these functions at very short correlation distances. This feature may be generally regarded as an indication of H-bonding in associated fluids. However, previous MD studies of SCW[21] have shown that the above consideration could not be absolutely accurate to imply the existence of H-bonding in the fluids. The authors in that study pointed out that the absence of a sharp peak at very short distances in the $g_{H-O}(r)$ function of SCW does not, in general, suggest the absence of H-bonding in the fluid. Therefore, since H-bonding is the primary process which leads to aggregation phenomena in scEtOH indicated by spectroscopic measurements, one needs to perform an analysis on each configuration of the system on the basis of a relevant

and rigorous criterion in order to estimate accurately the number of H-bonds between different molecules.

Following the literature, we can see that various models on the basis of energetic and geometric criteria have been used in CS studies so far to search the degree of H-bonding in dense molecular systems.[15,18,24,25,27] In an energetic approach, two molecules are considered to be H-bonded if their pair interaction energy is larger than a limiting value U_{lim}. Alternatively, hydrogen bonds can also be defined in a purely geometric way by conditions concerning the O···O and O···H separations of the two molecules and with an angle characterizing the geometry of the hydrogen bond, for example, the H−O···O angle.

Note also that in some cases this seems to favor a combination of an energetic with a geometric criterion in order to provide certain results of the H-bonding, as Kalinishev pointed out in the case of SCW.[19,22] However, in the case of pure liquid alcohols, the choice of a criterion is less crucial than that for other liquids such as water and both energetic and geometric criteria provide similar results.[16,53]

As in previous H-bonding studies of liquid alcohols[57,58] and in our MD simulation of scMeOH,[53] we have adopted here a rather strict geometric definition. Our choice for the above criterion was based upon the behavior obtained for the most relevant relative to the H-bonding first peaks of H−O and O−O pdf's of EtOH at SC conditions under study. It is due to the fact that H-bonding includes interatomic configurations of the following general type

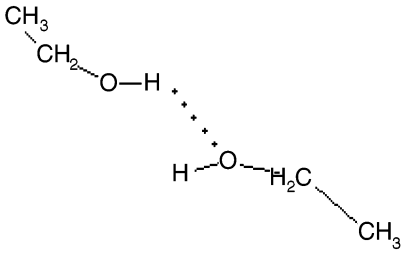

Note that the H-bonding peaks in these correlations at SC conditions are found to be not diffuse as in the case of the O−H pdf of SCW.[34]

Thus, a H-bond between two EtOH molecules at these SC conditions exists if their interatomic separation O···O and O···H is less than 3. 8 and 2.7 Å respectively, and the angle H−O···O, Φ, is smaller than a fixed limiting angle $\Phi^C = 30°$. The cutoff distances O···O and O···H are taken to be the average distances of the first minimum locations in the $g_{OO}(r)$ and $g_{HO}(r)$ pdf's, respectively.

As in our previous studies,[27,28,53,56] we have examined the angular variation of such bonds in order to find the limiting angle Φ^C. The results obtained have shown that in all cases the total number of H-bonds does not scale for angles greater than $\Phi = 30°$. Moreover, the position of the first minima of the functions $g_{OO}(r)$ and $g_{OH}(r)$ does not show important changes at these SC conditions, especially in the case of the $g_{OH}(r)$ value from which we determined the most critical cutoff value of the distance O···H (see subsection 3.1). Thus, we employed the same H-bond definition in all MD simulations at SC state points of interest. Note, however, that in the case of liquid EtOH our geometric H-bonding criterion was somewhat different compared to that employed to study the SC fluid. In this case, the results from a similar procedure led us to select the distances of 3.5 and 2.6 Å as the cutoff distances for the closest interatomic separations O···O and O···H, respectively.

It is interesting to mention here that some supplementary work has been also carried out in order to examine the reliability of another energetic criterion proposed by Jorgensen[15] in a previous Monte Carlo simulation study of the liquid system. Our results obtained on the basis of energetic and geometric criteria at 298 K (ambient EtOH) are found to be in good agreement with those obtained by Jorgensen et al.,[15] and by Saiz et al.[58] using the same geometric definition as in our study.

TABLE 1: Simulated Supercritical and Liquid State Points of Ethanol and Thermodynamic Results Derived from This NVT-MD Study

	experimental[60]			simulation			
state	T (K)	P (MPa)	ρ (g/cm^3)	T (K)	P (MPa)	$-U_p$ (kJ/mol)	D (10^{-9} m^2 s^{-1})
A	523	10.0	0.464	523.1	6.64	17.23	32.12
A1	523	2.0	0.0216	523.1	2.79	−0.384	866.96
A2	523	6.4	0.130	523.1	5.90	5.844	166.21
A3	523	15.0	0.523	523.1	12.60	19.14	25.42
B	523	20.0	0.566	523.0	21.51	20.42	21.80
C	523	30.0	0.602	523.1	35.10	21.61	20.75
D	623	10.0	0.132	623.1	10.16	3.21	195.25
E	623	20.0	0.339	623.1	20.12	10.13	66.19
F	623	30.0	0.447	623.1	31.42	13.39	38.02
G	723	10.0	0.090	723.1	10.03	0.59	302.65
H	723	20.0	0.207	723.1	20.72	4.34	133.86
I	723	30.0	0.312	723.1	31.89	7.49	80.91
liquid	298	0.1	0.787	298.15	0.21	39.51	1.34

Moreover, in the framework of the present treatment a detailed statistical analysis[58] of different configurations of the simulated fluid was carried out in order to study the H-bonded chain clusters (oligomers) in the system. With the aim to obtain qualitatively a visual picture of the H-bonding phenomenon and possible molecular aggregates in the fluid, we have constructed some animations using the MD produced trajectories of the fluid. Note also that some snapshots of individual configurations (see Figures 10 and 11) were selected emphasizing the existence of some oligomers identified in the sample throughout the implementation of the H-bonding search procedure. Finally, the results obtained are presented and discussed below.

2.3. Molecular Dynamics Simulation Details. In this treatment, the MD simulations of scEtOH were carried out at various SC thermodynamic conditions for which experimental (PVT) data are available in the literature.[60] All the state points studied here are listed in Table 1. Thus, we performed 12 NVT-MD simulations of the fluid at corresponding thermodynamic states and a further simulation at ambient conditions. Note that two of these MD runs at 523 K concern the lowest densities of the fluid studied (0.0216 and 0.130 g cm^{-3}) corresponding to pressures of 20 and 64 bar. The simulations were performed with 256 EtOH molecules in a cubic simulation box using standard periodic boundary conditions. Trial runs with 500 molecules in the simulation box have been also carried out, and the results obtained are found to be almost identical to those with 256 molecules.

Each EtOH molecule was modeled by four site interactions including also torsional motion. Thus, there was one site on each atom, namely, the O and H atoms of the hydroxyl group, while the CH_3 and CH_2 groups were considered as single interaction units centered on carbon. Note also that bond lengths and bond angles on the molecule were kept constant, and the only intramolecular motions considered during the simulations are torsions around the C−O bond. The interactions between sites of different species are described by a short-range Lennard-Jones (12−6) (LJ) part and a long-range Coulombic term. A full cutoff radius ($r_c = L_{box}/2$) was applied to all LJ interactions between the molecules of the fluid.

We adopted the molecular geometry and the potential parameters proposed by Jorgensen (see Table 2 in ref 15). The

TABLE 2: Positions and Heights of the First Maximum in the pfd's (r (Å), $G(r)$) of the SC (MD runs A−I) and Liquid Ethanol[a]

state	$g_{com}(r)$	$g_{O-O}(r)$	$g_{O-H}(r)$	$g_{H-H}(r)$
A	4.67/1.49/9.14	2.82/2.26	1.92/2.02	2.52/2.26
A1	4.39/2.72/0.82	2.82/6.95	1.92/6.13	2.52/6.43
A2	4.62/1.95/3.93	2.85/3.71	1.92/3.19	2.48/3.66
A3	4.67/1.47/10.71	2.85/2.20	1.99/1.99	2.48/2.19
B	4.67/1.47/10.52	2.82/2.15	1.92/1.94	2.48/2.15
C	4.67/1.47/10.91	2.82/2.12	1.92/1.92	2.48/2.13
D	4.71/1.61/3.30	2.87/1.88	1.97/1.55	2.53/1.93
E	4.71/1.48/7.23	2.87/1.56	1.97/1.30	2.53/1.62
F	4.71/1.45/8.87	2.83/1.47	1.97/1.23	2.53/1.54
G	4.85/1.49/2.06	2.97/1.22	2.12/0.95	2.62/1.31
H	4.95/1.45/4.85	2.93/1.14	2.07/0.89	2.57/1.24
I	4.85/1.43/7.26	2.92/1.10	2.02/0.87	2.57/1.19
liquid	4.48/1.48/13.50	2.73/5.05	1.83/5.33	2.43/4.31

[a] The third column values in the $g_{com}(r)$ are the first shell coordination numbers, $\{\langle n_i \rangle - 1\}$,computed using eq 1.

TABLE 3: Correlation Times τ of the First (P_1) and Second (P_2) Legendre Polynomial ACFs of the Unit Vector along the C−O and O−H Bonds as Well as along the Dipole Moment $\vec{\mu}$ of the Ethanol Molecule Obtained from This Study at SC Conditions

	bond C−O		bond O−H		dipole $\vec{\mu}$	total dipole $\vec{M}$
state	τ_1 (ps)	τ_2 (ps)	τ_1 (ps)	τ_2 (ps)	τ_1 (ps)	τ_D (ps)[a]
A	0.56	0.23	0.51	0.23	0.48	0.67
A1	0.36	0.26	0.18	0.10	0.16	0.15
A2	0.31	0.27	0.23	0.11	0.23	0.31
A3	0.59	0.25	0.56	0.25	0.52	0.77
B	0.63	0.27	0.59	0.27	0.53	1.04
C	0.68	0.28	0.64	0.29	0.59	0.90
D	0.22	0.15	0.14	0.07		
E	0.29	0.16	0.21	0.10		
F	0.34	0.17	0.26	0.12		
G	0.19	0.15	0.10	0.06		
H	0.20	0.13	0.12	0.06		
I	0.21	0.14	0.13	0.07		

[a] τ_D is the simulated Debye correlation time of the total dipole moment $\vec{M}$ of the system.

LJ cross interaction parameters are obtained using the geometric mean for both σ and ϵ. Also, the long-range electrostatic interactions were treated using the Ewald summation method with conducting boundary conditions.[61]

The partial local charges and molecular geometry used produce an effective dipole moment of 2.22 D (1 D = 3.335×10^{-30} C cm), which is substantially larger, compared to the experimental gas-phase value of 1.69 D.[62] The main reason for this is to account for the mutual polarization effects, which cannot be neglected in dense media.

Our choice for this optimized potential (OPLS) is based on the results from previous and present simulation studies on liquid EtOH, which have shown that the aforementioned potential reproduces quite well the properties of the liquid. Moreover, it is particularly important here to check the accuracy of this potential in predicting the properties of the system at SC conditions.

In addition to the short-range LJ and long-range Coulombic interactions, torsional energy was taken into account expressed by the following potential function (see Table 3 in ref 15)

$$V(\phi) = V_0 + \frac{1}{2}V_1(1 + \cos\phi) + \frac{1}{2}V_2(1 - \cos 2\phi) + \frac{1}{2}V_3(1 + \cos 3\phi) \quad (2)$$

The equations of motion were integrated using a leapfrog-type Verlet algorithm with the Berendsen and co-workers thermostat.[63] Furthermore, constraints for bond length and bond angles were handled during the simulations by using the SHAKE method.[64] The time step was 1 fs. At each thermodynamic state point we carried out two MD runs. The first one has been extended to about 300 ps in order to achieve equilibrium. The second period of 400 ps was used to calculate all the properties of interest in the thermodynamic equilibrium.

3. Results and Discussion

The most important thermodynamic properties of SC and liquid EtOH obtained from the present NVT-MD simulations are summarized in Table 1. The calculated properties are the mean configurational energy, $U_p = U_{inter} + U_{intra}$, the pressure, P, and the self-diffusion coefficients of the fluid at different conditions. As it becomes apparent from Table 1, the comparison of the simulated and experimental pressures shows reasonable agreement almost at each thermodynamic state point investigated in this study. The heat of vaporization ΔH_{vap} is estimated from the relation

$$\Delta H_{vap} = U_{intra}(\text{gas}) - [U_{intra}(\text{liq}) + U_{inter}(\text{liq})] + RT \quad (3)$$

For the liquid EtOH at 298 K and normal pressure, we have obtained a ΔH_{vap} value of 42.89 kJ/mol, which is in quite good agreement with that of the experiment ($\Delta H_{vap}^{exp} = 42.3$ kJ/mol).[65] Additionally, we performed trial NVT-MD simulations of the liquid at $T = 298$ K and normal pressure by employing the OPLS all-atom (AA) force field.[66] This particular force field is a nine-site potential model, which includes harmonic bond stretching, angle bending, and anharmonic dihedral potentials in terms of a Fourier series as well as Coulombic plus Lennard-Jones terms for inter- and intramolecular nonbonded interactions. The results obtained support our conclusions that, more or less, the accuracy of the simple united atom OPLS model in comparison with the results from the more analytic potential model OPLS AA and with experiment is relatively good. Furthermore, it is very important to mention here that the united atom OPLS model used in this study is less demanding in CPU time compared to the OPLS AA one. Finally, the self-diffusion coefficients of the molecules have been calculated by using the molecular com mean square displacements. The results obtained show a very strong density dependence under these SC conditions as expected.

3.1. Intermolecular Structure. Let us now investigate the intermolecular structure of scEtOH in terms of various site−site pdf's calculated at each state point of interest.

The com−com pdf's are shown in parts b−d of Figure 1 together with the corresponding function for the liquid at ambient conditions displayed in Figure 1a. Also, the characteristic extrema (positions and heights of the first peak) of these pdf's are summarized in Table 2. From Figure 1a it is seen that the com−com function exhibits a first peak around 4.76 Å followed by a distinct second and third broad peak at 8.5 and 12.7 Å, respectively. This result reveals the typical behavior of liquids as expected. In contrast to the com−com pdf for the liquid, the corresponding functions at SC conditions show a noticeable different behavior. The intensity of the second peaks in these functions appears to be strongly reduced while the third peak is not apparent. We may also observe some small dependence of the first peak amplitude with temperature at constant pressure and vice versa. By comparing these functions

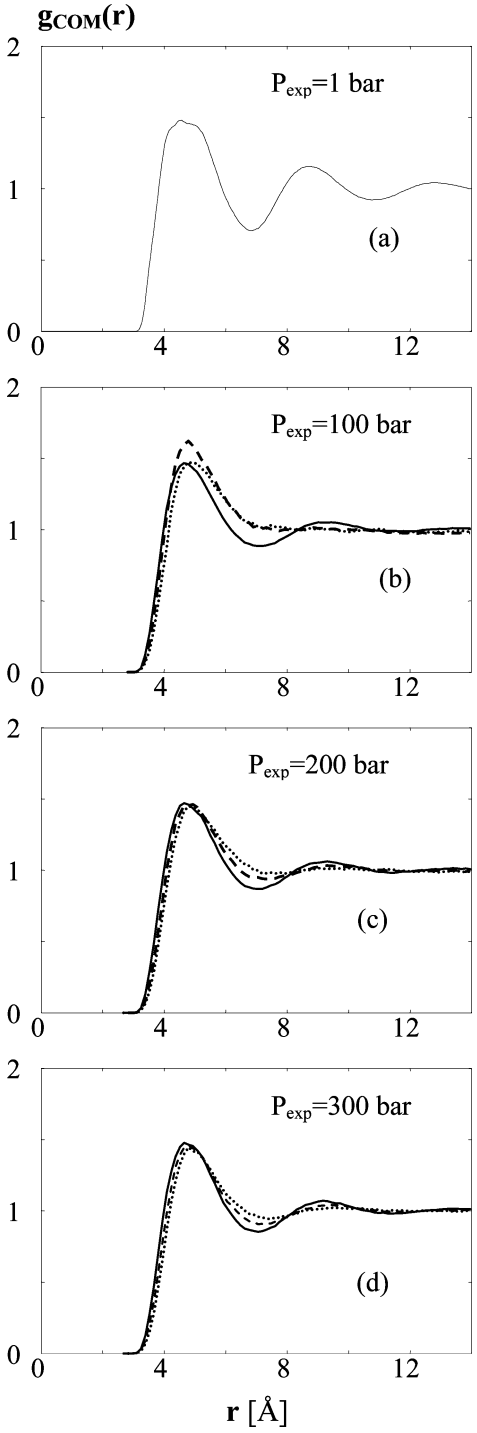

Figure 1. Center of mass pair distribution functions of liquid ((a) T = 298 K, P = 1 bar) and superctitical (b, c, d) ethanol at nine thermodynamic conditions: — (T = 523 K), - - - (T = 623 K), ··· (T = 723 K).

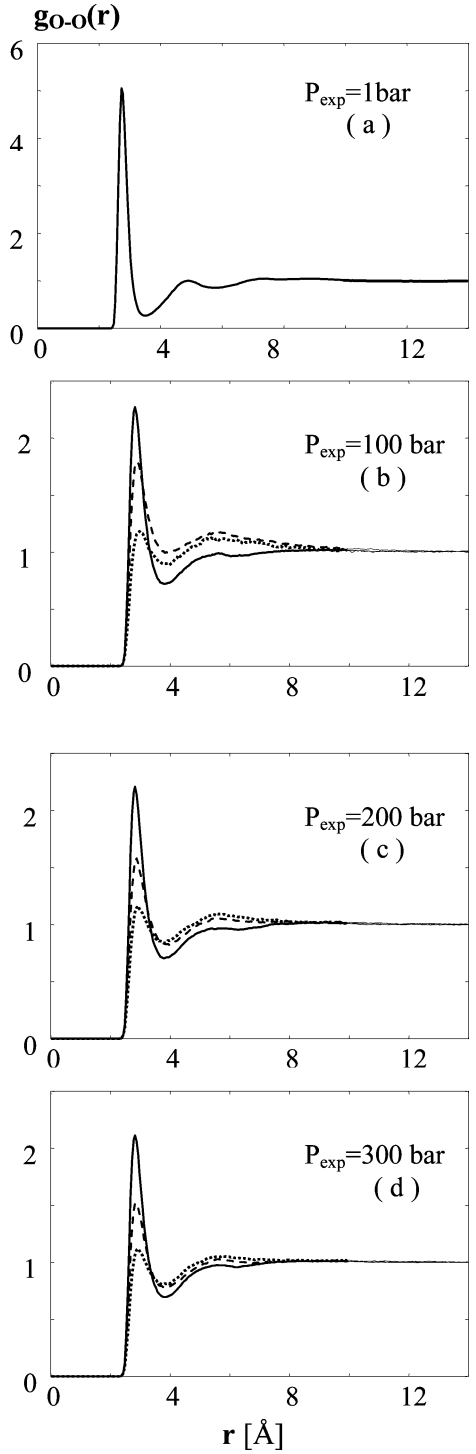

Figure 2. Site−site pair distribution functions for O−O of liquid ((a) T = 298 K, P = 1 bar) and superctitical (b, c, d) ethanol. The symbols in parts b, c, and d are the same as in Figure 1.

with the com−com pdf's of scMeOH at exactly the same conditions (see Figure 1 in ref 53), we can easily observe remarkable differences with regard to the shape of these functions at relatively short intermolecular distances up to 5 Å. In the case of scMeOH, the short-range part of these pdf's exhibits two overlapping peaks. As pointed out in ref 53, this feature reflects clearly the fact that scMeOH remains highly structured at these conditions. On the other hand, a similar qualitative conclusion cannot be drawn for the behavior of scEtOH on the basis of the corresponding com−com pdf's. We shall see below that a similar result is also obtained for the structure of this fluid by analyzing the most appropriate atom−atom pdf's of the system.

To gain additional insight into the microscopical structure of scEtOH, the site−site pdf's O−O, H−H, H−O, and Me−H have been computed and analyzed. These functions are shown in Figures 2−5. The corresponding functions for the liquid EtOH are also presented for comparison purposes. The positions and heights of the first peak of these pdf's are summarized in Table 2. It should be noted here that these correlations are in quite good agreement with those reported in previous CS studies of this liquid.[15,58] As it can be seen from the behavior of the

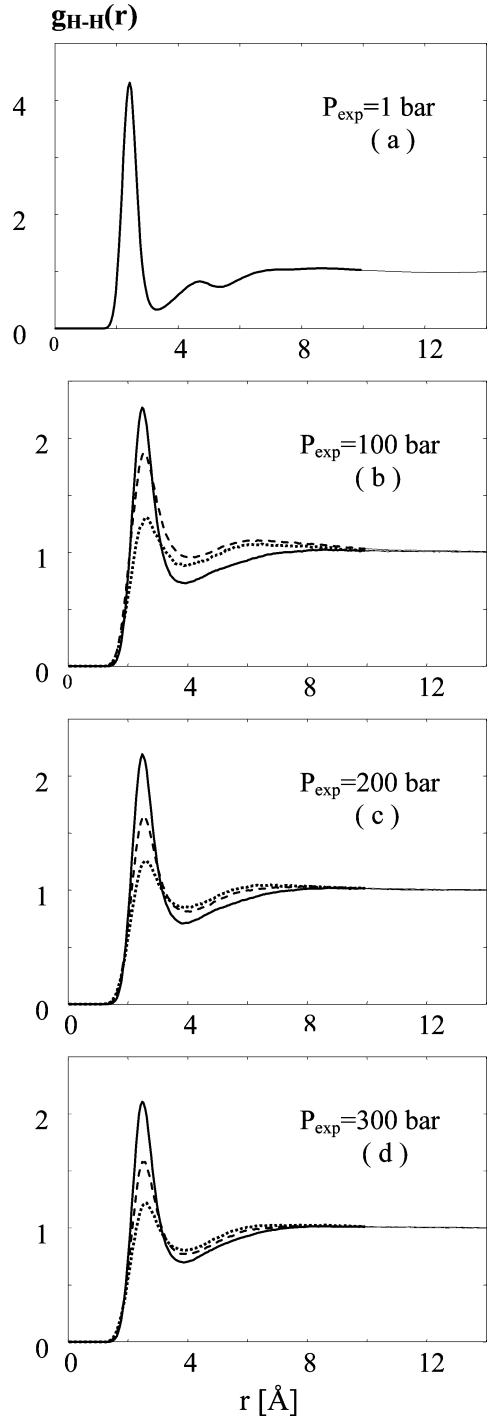

Figure 3. Site−site pair distribution functions for H−H of liquid ((a) $T = 298$ K, $P = 1$ bar) and superctitical (b, c, d) ethanol. The symbols in parts b, c, and d are the same as in Figure 1.

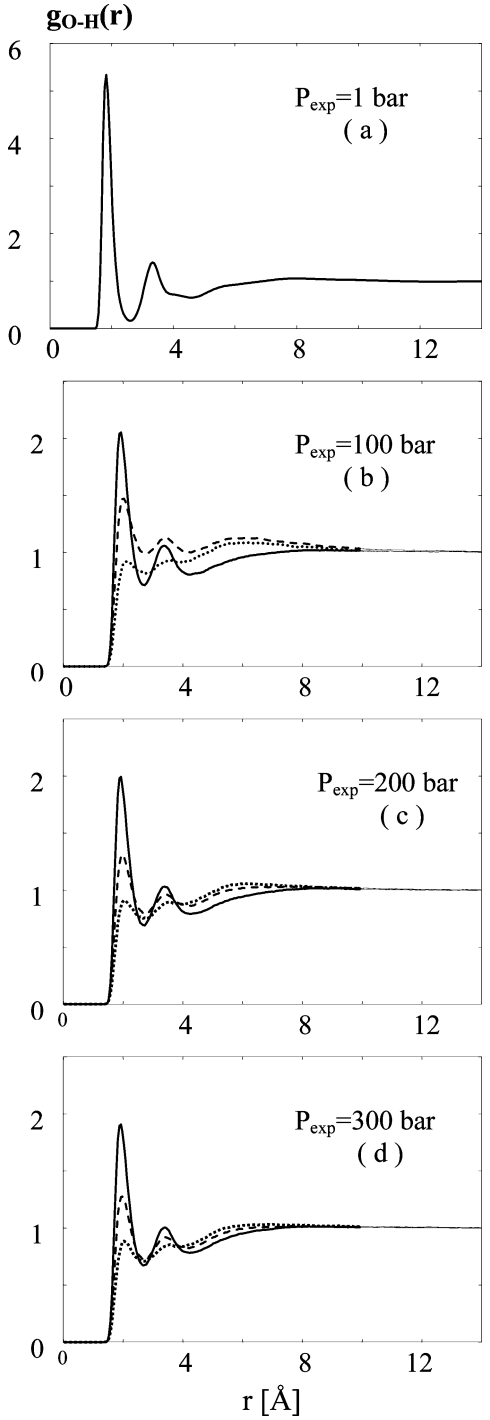

Figure 4. Site−site pair distribution functions for O−H of liquid ((a) $T = 298$ K, $P = 1$ bar) and superctitical (b, c, d) ethanol. The symbols in parts b, c, and d are the same as in Figure 1.

aforementioned functions and the data selected in Table 2, the trends observed in the pdf's for the liquid are also observed in the corresponding functions for the fluid at SC conditions. On the other hand, the O−O, H−H, and H−O curves show a prominent sharp first peak followed by a distinct minimum at short intermolecular distances. In the case of the Me−H pdf's, the first peaks observed are relatively small in height and exhibit a more diffuse shape. Another interesting feature is that the first peak positions in O−O, H−H, and H−O functions are slightly affected by temperature and pressure. Also, the decrease of the corresponding amplitudes of the peaks in these functions seems to be more significant with temperature than with pressure. Generally, it becomes apparent from Figures 2−4 that the amplitudes of the first peak in the H−H, O−O, and H−O pdf's of scEtOH near the critical point (states: A, B, C) remain relatively high compared to the pdf's of the liquid. The sharp first peaks observed in these functions reflect the existence of H-bonds between molecules in the fluid. This H-bonding sign in scEtOH may be also supported by the behavior of the O−O and especially that of the H−O function in contrast to the H−H correlation. Concretely, as in the case of scMeOH,[45,53] the O−O and O−H pdf's in scEtOH are also more structured than the H−H function. These functions exhibit a very strong sharp first peak followed by a deep minimum and further by a distinct

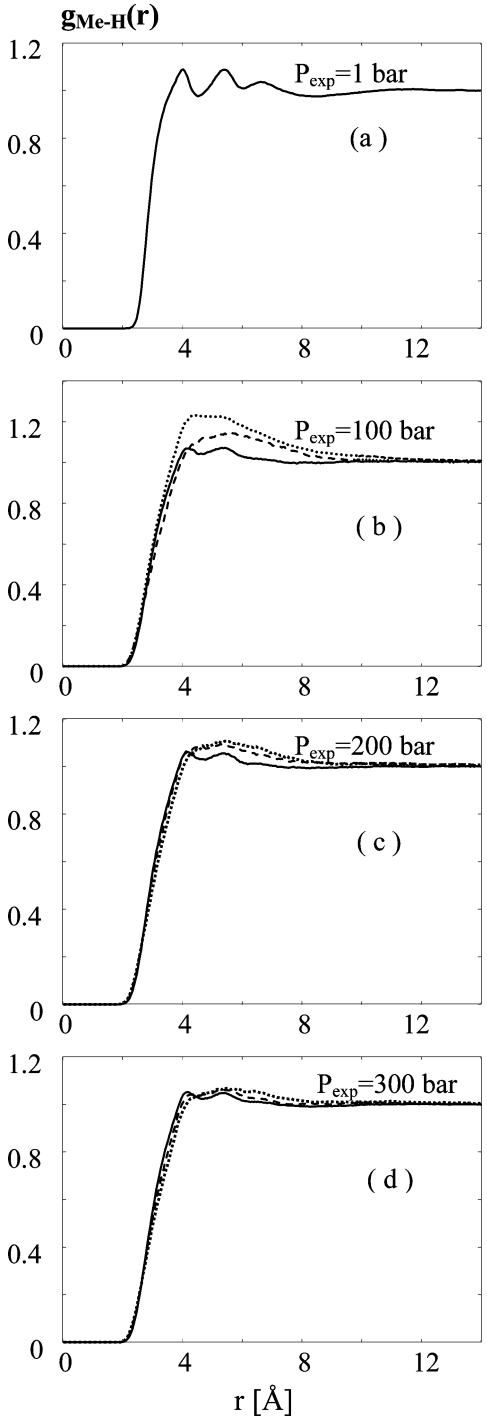

Figure 5. Site−site pair distribution functions for Me−H of liquid ((a) $T = 298$ K, $P = 1$ bar) and superctitical (b, c, d) ethanol. The symbols in parts b, c, and d are the same as in Figure 1.

second maximum, which for the most state points under study has to be compared with the amplitude of the first peak in H−H and com−com functions. Note also that in contrast to the O−H pdf's, the second peak in the O−O pdf's appears to be rather shallow with a maximum near 5.0 Å. It is clear that this distinct second maximum in these functions reflects the formation of a second solvation shell around the O atom. Consequently, at these SC conditions, this result strongly suggests that scEtOH still remains structured.

Another point of interest is the ordering observed for the first peak locations of the site−site pdf's. We found that this correlation distance increases in the following order: $r_{HO} < r_{HH} < r_{OO} < r_{MeH} < r_{MeMe}$. Therefore, from the overall behavior of the site−site pdf's we may conclude that the EtOH molecules at SC conditions in the first solvation shell tend to reorient their H atoms very close toward the O atom of the central molecule, whereas the hydrophobic Me···Me separation was found to be the greatest when compared to the rest of the intermolecular site−site separations. Moreover, the presence of the first sharp peak in the H−O functions at extremely short correlation distances followed by a deep minimum at an almost invariant distance in the SC region may be regarded as a manifest of H-bonding.

Finally, the reliability of all the structural results obtained in the framework of the present study should be judged by an imperative comparison with suitable real experimental data. It is well-known that ND experiments with hydrogen/deuterium isotope substitution are suitable in principle to predict structural data on molecular fluids. Since, however, ND studies on scEtOH have not been performed so far, a definitive solution of the problem of the microscopical intermolecular structure of this fluid cannot be given at the present time.

3.2. Reorientational Dynamics. Generally, for the study of the dynamical properties of dense fluids, it is convenient to assess and analyze the appropriate time correlation functions (tcf's) of the relevant dynamical variables of the system under investigation. In the course of the present MD study, we have calculated the tcf's corresponding to the single and collective particle dynamical properties of the system. In this part of our treatment, we present and discuss the results obtained for reorientational dynamics of the fluid in conjunction with recently available NMR and dielectric experimental data from the literature.

The reontientational dynamics of the molecules in the fluid are studied in terms of the first- and second-order Legendre reorientational tcf's, $C_L(t)$, defined by the following expressions

$$C_L^x(t) = \langle P_L(\hat{u}_x(0)\cdot\hat{u}_x(t))\rangle, \quad x = a, b, \mu; L = 1, 2 \qquad (4)$$

$\hat{u}_a$, $\hat{u}_b$, and $\hat{u}_\mu$ are the bond unit vectors O−H, C−O, and the dipole moment of the molecule, respectively.

The results for the first- and second-order Legendre tcf's, namely, $C_1^{C-O}(t)$ and $C_1^{H-O}(t)$ and $C_2^{C-O}(t)$ and $C_2^{H-O}(t)$, at each thermodynamic state of interest, are shown in Figures 6 and 7, respectively. All the aforementioned tcf's have been compared to each other, and the estimated correlation times are summarized in Table 3. In any case, to estimate the corresponding correlation time, we have employed a combined method. According to this method, we used a numerical integration up to a short time (nondiffusive part of the tcf) and fitted the rest of each tcf to an exponential function. Thus, we obtained analytically the integral for the rest of the tcf from the fit. The sum of these two calculated times corresponds to the aforementioned correlation time of the tcf under investigation.

In what follows, we will first discuss the behavior of the O−H tcf's with temperature at constant pressure and vice versa. As mentioned above, Besnard and co-workers[51] reported vibrational spectroscopical studies of pure scEtOH combining the IR and Raman techniques. Their work was based on the O−H stretching vibration mode as a very sensitive group of the molecule participating in H-bonding. We have therefore chosen to study the reorientational tcf's of the hydroxyl group due to the fact that the $C_1^{H-O}(t)$ correlation is related to the IR measurements and $C_2^{H-O}(t)$ to the Raman and NMR.

By inspecting the predicted correlation times τ_1^{H-O} and τ_2^{H-O} from Table 3, we may observe that at each state point (A−I)

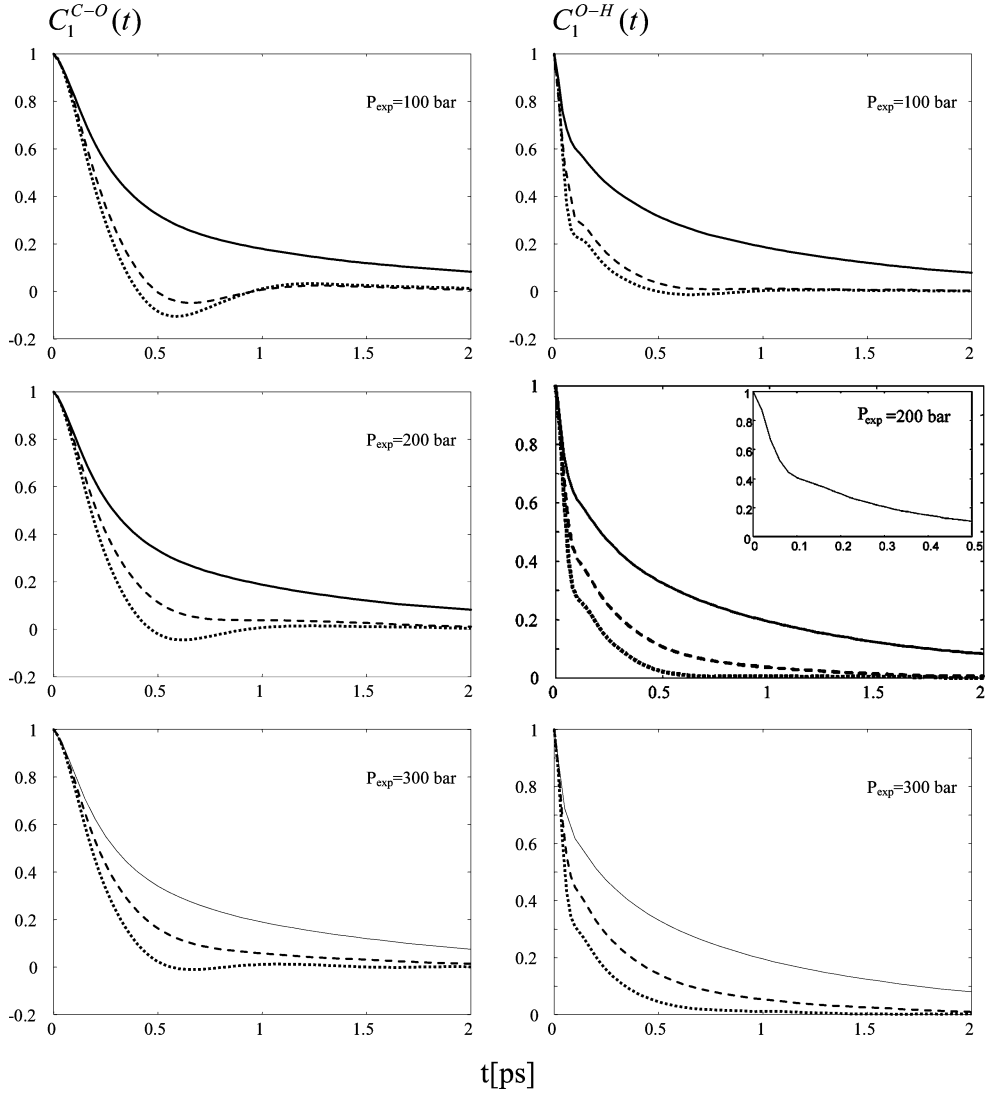

Figure 6. First-order Legendre time reorientational correlation functions for the bond unit vector of C−O and O−H of superctitical ethanol at nine thermodynamic state points. The inset in the figure at $P = 200$ bar corresponds to the same curve at 523 K shown up to 0.5 ps. The symbols are the same as in Figure 1.

the time τ_1^{H-O} appears to be greater than the τ_2^{H-O} one, as expected. In addition, it is clearly seen that the well-known Hubbard[67] relation ($\tau_1 = 3\tau_2$) is not fulfilled at these conditions. In other words, the reorientational motion of the hydroxyl group of the molecule might be characterized as not an absolutely diffusional one. Previous experimental and theoretical studies on several self-associated liquids have led to the conclusion that especially the reorientational dynamics of such systems are considered to be strongly sensitive to the microscopic H-bonding interactions. In liquids, for instance, the reorientational relaxation process is usually observed in the well-known diffusive regime, while at SC conditions and for low density the corresponding tcf's generally display a somewhat different behavior as in the case of scMeOH[44] and scEtOH.

As we can see from Table 3, the pressure dependence at constant temperature of the predicted correlation times τ_1^{H-O} and τ_2^{H-O} is substantially small. Note, for instance, that there are marginal differences between the values of τ_1^{H-O} or τ_2^{H-O} on going from 10 to 30 MPa of pressure at a fixed temperature of 523, 623, or 723 K. On the other hand, the temperature dependence at constant pressure of these correlation times is found to be quite significant. The values obtained for the correlation times decrease drastically at constant pressure with increasing temperature. This is of course due to the collapse of the H-bonding network with the decreasing density of the system as it is also confirmed by the H-bonding analysis presented below and by the recently reported NMR studies.[44] Concretely, in that study the single-molecule reorientational relaxation of the deuterated scMeOH and scEtOH was investigated on the basis of ^{2}H NMR spin−lattice relaxation measurements carried out at 543 K and different densities, ρ, up to 2 ρ_c. In the case of scEtOH ($T_c = 516$ K, $P_c = 6.4$ MPa, $\rho_c = 0.28$ g cm^{-3}), we have attempted to compare our MD τ_2^{H-O} reorientational times with those acquired from the aforementioned NMR study.[44] From the results shown in Figure 3 in that study, we see that the NMR τ_2^{H-O} times at 543 K are in the range 0.1−0.3 ps for densities in the region 0.05−2 ρ_c (0.014−0.56 g cm^{-3}) and it exhibits a minimum value of 0.1 ps around 0.2 ρ_c (0.056 g cm^{-3}). Our MD τ_2^{H-O} reorientational times (see Table 3) for 523 K and state points A−C (0.464−0.602 g cm^{-3}) are in the range of 0.23−0.29 ps, which are in quite good agreement with those from NMR in the high-density region. Moreover, three supplementary MD runs at 523 K and densities 0.0216, 0.130, and 0.523 g cm^{-3} provided τ_2^{H-O} reorientational times of 0.10, 0.12, and 0.25 ps, respectively, which when compared to the

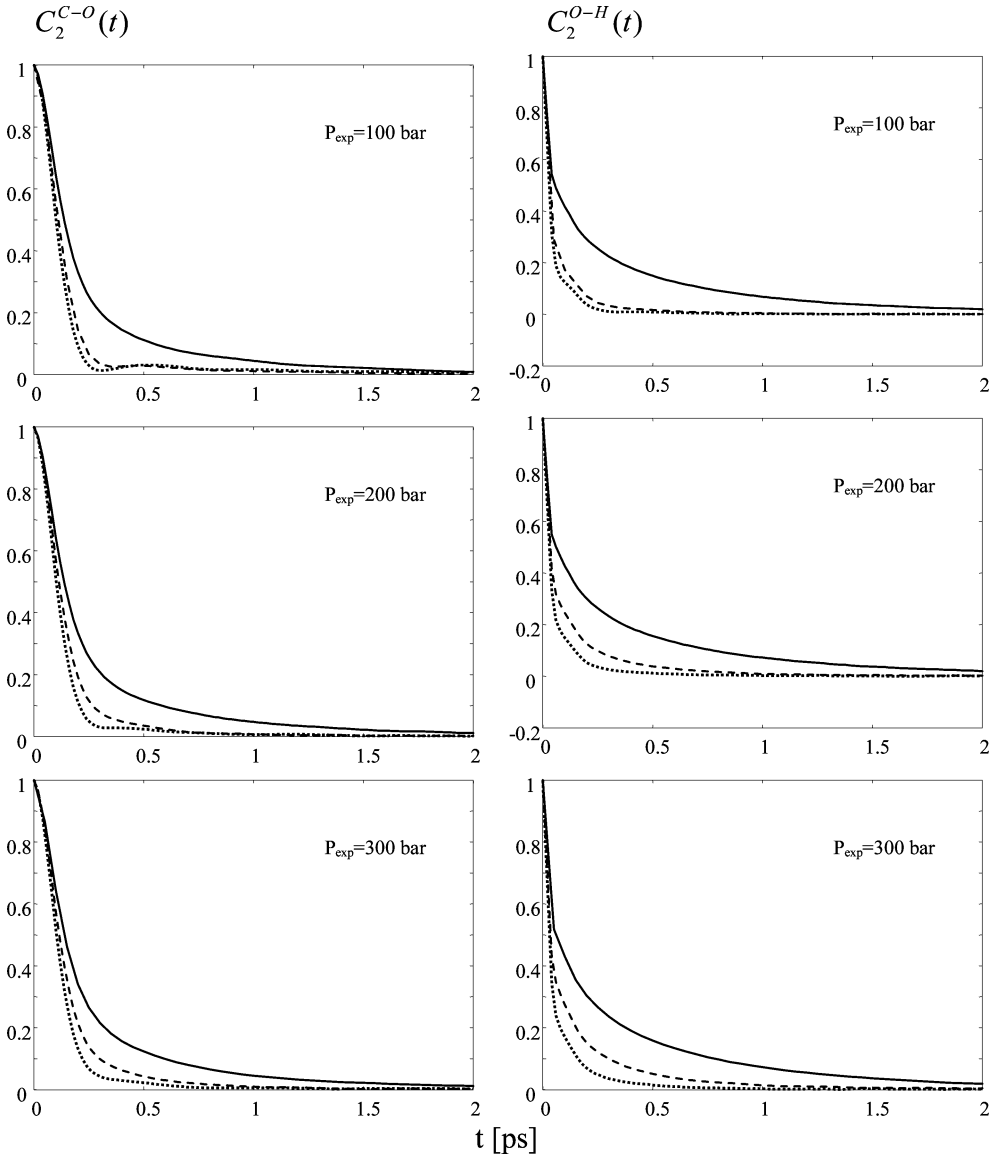

Figure 7. Second-order Legendre time reorientational correlation functions for the bond unit vector of C−O and O−H of superctitical ethanol at nine thermodynamic state points. The symbols are the same as in Figure 1.

experimental ones at the same densities were found to be in excellent agreement.

Another point of main interest here is the shape of the tcf's of the hydroxyl group. As we can see from Figures 6 and 7, the $C_1^{H-O}(t)$ and $C_2^{H-O}(t)$ correlations show a very fast decay and converge to zero approximately after 2 ps. In addition, at very short times (0.1−0.2 ps) these functions exhibit a well-formed shoulder, which usually is related to the librational motions occurring in associated systems due to the H-bonding network. A comparison of these tcf's with corresponding experimental results, especially with those from the IR and Raman[51] studies, is not possible at the present time because the acquired experimental tcf's have not been reported in that or in any other subsequent publication for scEtOH.

Further to the reorientational dynamics of the fluid, we have selected to study the reorientational motion of the bond unit vector C−O of the molecule as an attempt to explore the assumption that the rotational dynamics of this specific bond are less strongly affected by the local environment than the O−H dynamics. In fact, such a hypothesis has not been thoroughly investigated in previous studies of such molecular-like systems so far.

As in the case of the O−H dynamics, we may observe from Table 3 that at each state point (A−I) the predicted correlation time τ_1^{C-O} appears to be greater than the corresponding τ_2^{C-O} one. It is also clearly seen that the well-known Hubbard relation is not fulfilled. Note also that at each state point (A−I) the correlation time τ_1^{C-O} appears to be somewhat greater than the corresponding τ_1^{H-O} one. On the other hand, at each state point in the high-density region (A−C), the time τ_2^{c-o} appears to be almost identical compared with that of H−O, while τ_2^{c-o} is greater than τ_2^{H-O} at the state points in the low-density region (D−I). In addition, it should be mentioned here that at a very short time the tcf's for C−O do not exhibit the well-formed shoulder observed in the H−O correlation as discussed above.

Generally, from the above considerations and the decay of the tcf's C−O and H−O, we may conclude that the reorientational dynamics of the C−O bond unit vector are slower than that of the flexible O−H one, as expected. However, this different behavior changes strongly with density. Clearly, it seems that the density dependence of the O−H dynamics is larger than that of the C−O bond on going from the low- to high-density region of the fluid. This somewhat different

behavior between the C−O and O−H reorientational dynamics with density might be attributed to the H-bonding strength at higher densities in the fluid.

Finally, we have also attempted to estimate the dielectric properties of the system such as the static dielectric constant $\epsilon(0)$ and the Debye relaxation time τ_D.[68] The method we have employed to obtain these properties was based on the accurate calculation of the total dipole moment tcf, $C_M(t)$

$$C_M(t) = \frac{\langle \vec{M}(0)\cdot\vec{M}(t)\rangle}{\langle |\vec{M}(0)|^2\rangle} \quad (5)$$

$$\vec{M}(t) = \sum_{i=1}^{N} \vec{\mu}_i(t) \quad (6)$$

where $\vec{M}(t)$ is the total dipole moment of the sample at time t and $\vec{\mu}_i(t)$ corresponds to the permanent dipole moment of the molecule i.

It is known that the relation between the frequency-dependent dielectric permittivity $\epsilon(\omega)$ and the total dipole moment tcf $C_M(t)$ is given by the following equation[69]

$$\epsilon(\omega) = \epsilon_\infty + \frac{\rho}{3NK_B T\epsilon_0}\langle |\vec{M}(0)|^2\rangle[1 + i\omega A(\omega)] \quad (7)$$

where $A(\omega)$ is the Fourier transform ($A(\omega) \equiv \mathrm{FT}\{C_M(t)\}$) of the tcf $C_M(t)$, ρ the number density, and K_B Boltzmann's constant. ϵ_0 denotes the vacuum permittivity, whereas ϵ_∞ is the dielectric constant at optical frequencies ($\epsilon_\infty = 1$).

The static dielectric constant $\epsilon(0)$ at temperature T was calculated by using the following relation obtained from eq 7 at $\omega = 0$

$$\epsilon(0) = 1 + \frac{\rho}{3NK_B T\epsilon_0}\langle |\vec{M}(0)|^2\rangle \quad (8)$$

The Debye relaxation time τ_D has been calculated by means of the relation

$$\tau_D = \frac{1}{\langle |\vec{M}(0)|^2\rangle}\int_0^\infty \langle \vec{M}(0)\vec{M}(t)\rangle \, dt \quad (9)$$

We have used this method due to the fact that previous MD studies of polar fluids,[70−72] using Ewald sums with conducting boundaries, provided satisfactory results for the dielectric properties. Note however that the efficiency of the method depends on the simulation which must be long enough to estimate $\langle\{\vec{M}(0)\}^2\rangle$ and $C_M(t)$ precisely. In the present MD study, the calculation of the aforementioned properties was based upon a 1 ns long trajectory of the simulated scEtOH at 523 K and 100, 200, and 300 bar. The tcf's $C_1^\mu(t)$ and $C_M(t)$ at 523 K and 200 bar are shown in Figure 8, and the corresponding correlation times are given in Table 3. The MD results obtained for the static dielectric constant $\epsilon(0) = 4.2$ and the Debye relaxation time $\tau_D = 1.04$ ps at 523 K and 200 bar of scEtOH have been compared with available experimental data reported in a recent dielectric relaxation study by Hiejima and Yao.[50] The previous study for temperatures and pressures in the ranges 513−533 K and 14.8−22.3 MPa, respectively, provides experimental values for $\epsilon(0)$ (see Table 1 in ref 50) which are between 3.8 and 4.2. From the same table, the corresponding experimental τ_D times are in the range 4.6−4.1 ps.

In summary, our calculated dielectric properties $\epsilon(0)$ and τ_D lead us to conclude that the static dielectric constant shows a quantitative agreement with corresponding experimental data, while the Debye relaxation time from the simulation is somewhat shorter than that from dielectric measurements.

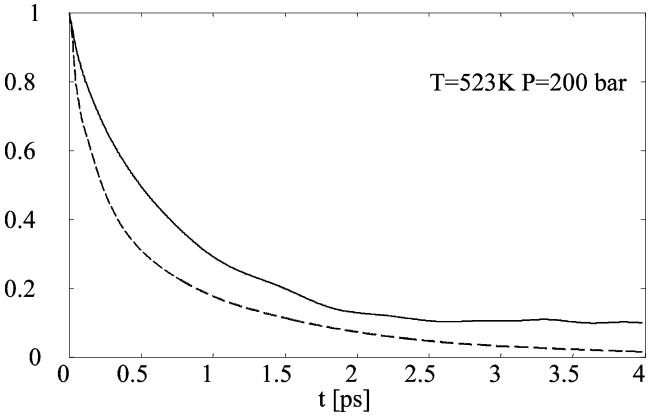

Figure 8. Time autocorrelation functions of the permanent dipole moment of the ethanol molecules (- - -) and the total dipole moment (—) of the sample at $T = 523$ K and $P_{exp} = 200$ bar.

TABLE 4: Hydrogen Bonding Analysis, Average Pencentage f_i of SC (states, A−I), and Liquid EtOH Molecules with *I* (0, 1, 2, 3, 4, ...)[a]

f_i	A	B	C	D	E	F	G	H	I	liquid
0	41.91	35.48	35.25	82.88	65.74	58.47	92.22	83.67	76.59	1.21
1	40.83	43.03	42.59	15.76	28.71	33.85	7.46	15.21	21.13	14.51
2	16.35	20.23	19.95	1.33	5.32	7.38	0.31	1.09	2.22	78.64
3	0.89	1.22	1.28	0.03	0.23	0.30	0.00	0.03	0.06	5.62
4	0.02	0.04	1.13	0	0.00	0.00	0.00	0.00	0.00	0.02
n_{HB}^{sim} [b]	0.81	0.88	0.89	0.17	0.40	0.49	0.08	0.17	0.25	1.89
n_{HB}^{exp} [c]	0.57	0.66	0.70	0.12	0.28	0.36	0.05	0.08	0.14	

[a] Hydrogen bonds and the average total number of H-bonds n_{hb}^{sim} per molecule from this NVT-MD study. [b] In order to directly compare the simulated with NMR experimental results one has to divide n_{HB}^{sim} by a factor of 2. [c] n_{HB}^{exp} corresponds to the hydrogen bonding degree of the system obtained from NMR experiment.[40]

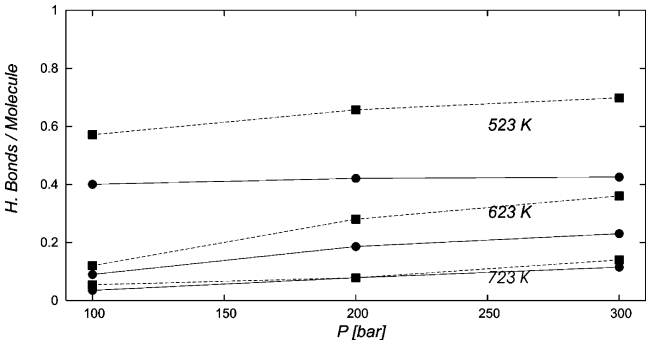

Figure 9. Degree of hydrogen bonding, $\langle n_{HB}\rangle$, as a function of pressure and temperature: — (MD this work), - - - (experimental[40]).

3.3. Hydrogen Bonding Analysis. Following the methodology described in subsection 2.2.2, and since the locations of the first minima of the pdf's $g_{OO}(r)$ and $g_{HO}(r)$ for scEtOH are found to be somewhat different from those obtained for scMeOH, we have chosen here a slightly different geometric criterion to that employed in our previous study.[53] Note also that we have employed the same H-bond criterion (see subsection 2.2.2) for MD runs at different state points (A−I). In addition, we defined the H-bonding state of a molecule according to the number of H-bonds that it exhibits. The number of H-bonds per molecule has been estimated independently on whether the EtOH molecule participates in a bond as a donor or acceptor.

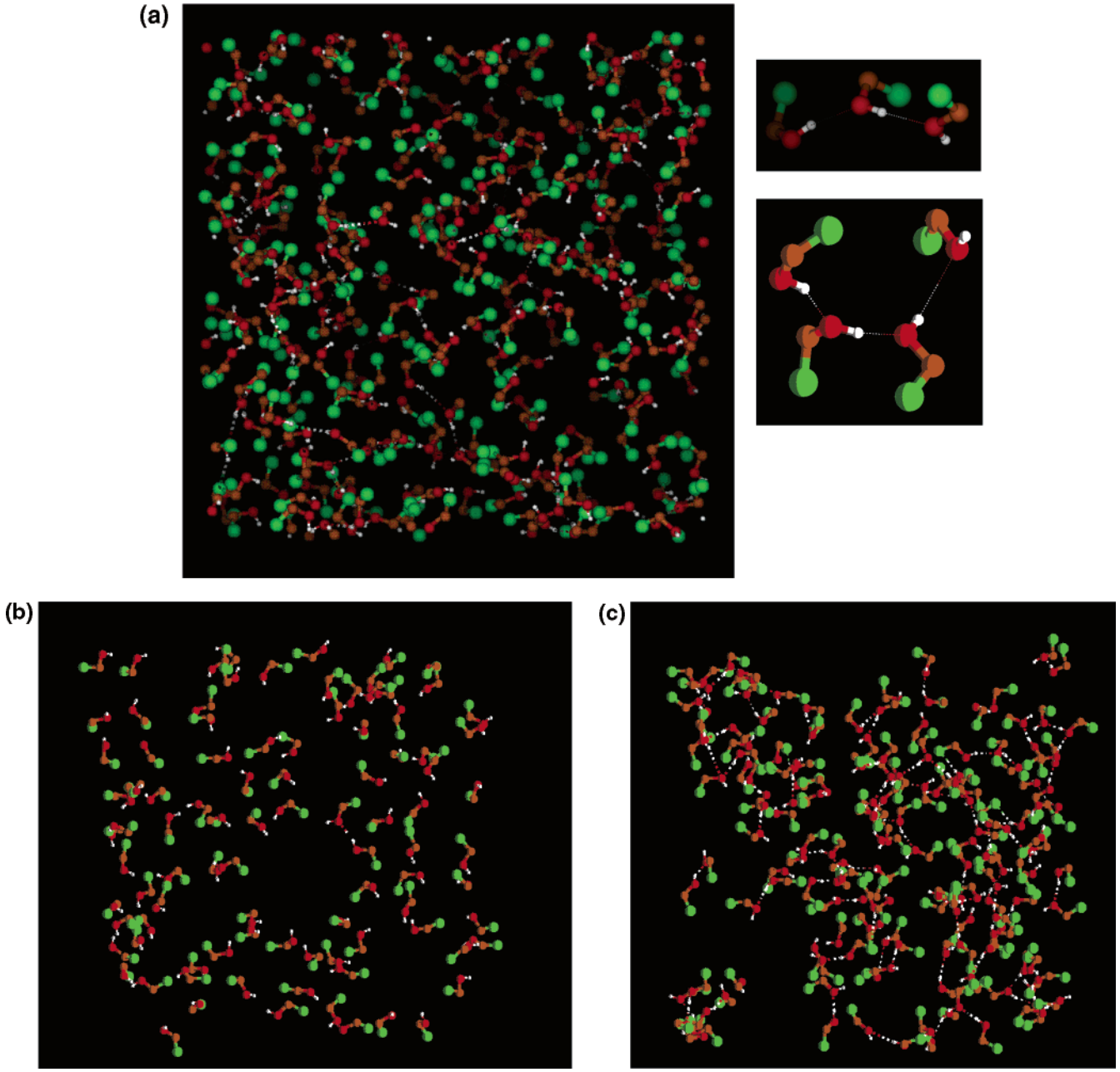

Figure 10. Snapshot of a representative configuration from this MD simulation of supercritical ethanol at $T = 523$ K and density corresponding to the pressure of 100 bar: (a) simulation box containing monomers, dimers, and other formed oligomers; (b) simulation box in which only the monomers are displaying; (c) simulation box in which only the hydrogen-bonded oligomers are shown.

As mentioned above, except the average number of H-bonds per molecule $\langle n_{HB} \rangle$ that has been predicted at each state point under study, we have also computed the percentage f_i of molecules with i ($i = 0, 1, 2, 3, ...$) bonds per molecule. Thus f_0 denotes the percentage of nonbonded molecules in the sample or monomer, f_1 the percentage of the molecules with one H-bond, etc. The method used to obtain the statistics f_i shown in Table 4 is exactly the same to that employed in our previous study for scMeOH[53] and in similar studies of H-bonding of liquid water and alcohols.[7,15−28] The average number of H-bonds per molecule may be calculated on the basis of the f_i statistics obtained. Additionally, we have estimated the percentage of free hydroxyl (O−H) groups according to the definition of Besnard and co-workers (p 3905 in ref 51). Thus, we have considered as free O−H groups in the sample not only the monomer (f_0-nonbonded) EtOH molecules but also the H-bond acceptor species at the ends of the open chain oligomers. Note also that in the framework of this study an analysis of different configurations of the simulated fluid was carried out to study the existence of possible H-bonded chain clusters (oligomers) in the system. The method used is similar to that of Saiz et al.[58] who studied H-bonded chains in liquid EtOH.

In the following paragraphs, we present and discuss our results. The results obtained for f_i ($i = 0, 1, 2, ...$) and the mean number of H-bonds per molecule are given in Table 4 together with experimental data reported by Hoffmann and Conradi.[40] In the same table, we also present our results for liquid EtOH at ambient conditions. As noted by these authors, the degree of H-bonding in scEtOH can be approximated using the observed chemical shift σ of the hydroxyl protons relative to the methyl resonance from their NMR measurements according to the linear relation $n = 0.205\sigma + 0.146$.

The degree of H-bonding obtained from the present MD study and experimental investigations[40] is also shown in Figure 9 as

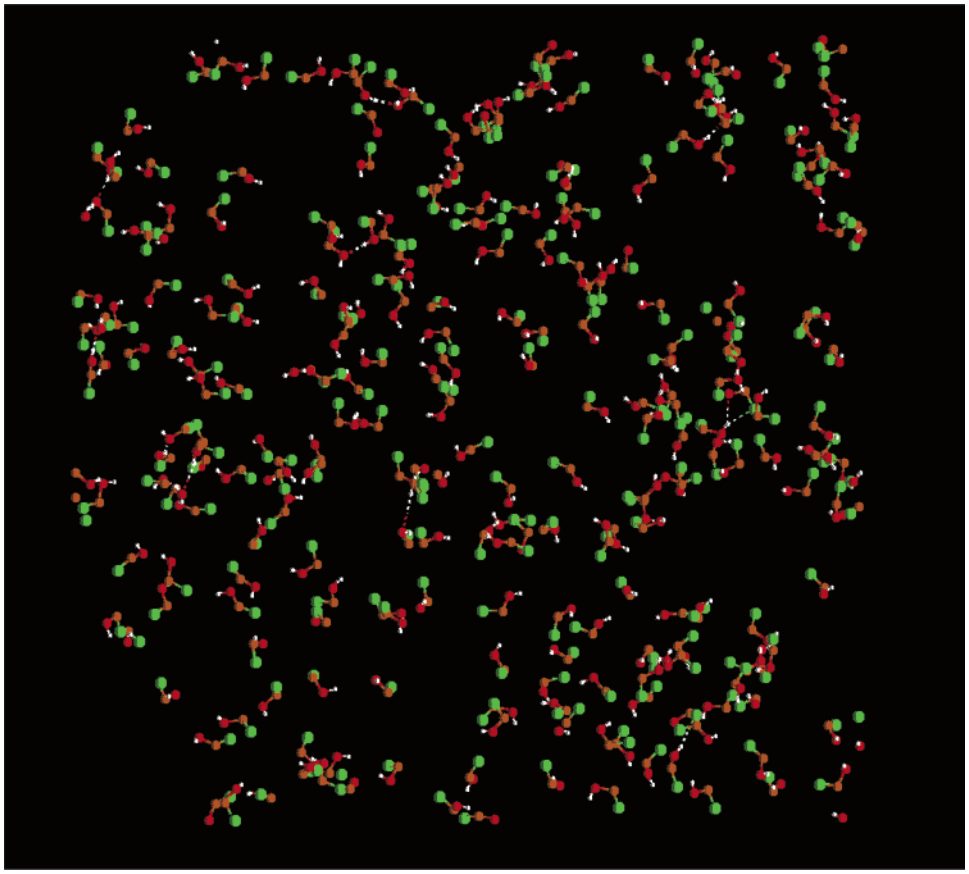

Figure 11. Snapshot of a representative configuration from this MD simulation of supercritical ethanol at $T = 723$ K and density corresponding to the pressure of 100 bar: The reduction of the hydrogen-bonding network at higher temperature is clearly shown.

a function of pressure and for 523, 623, and 723 K. As we may observe from Table 4 and Figure 9, the temperature and pressure dependence of $\langle n_{HB} \rangle$ from the NMR experiment was found to be qualitatively very similar to that of the simulation. A closer inspection of the results indicates that, as in the case of SCW[34] and scMeOH,[53] the decrease of the H-bonds in scEtOH is primarily temperature dependent. Moreover, the agreement between experiment and simulation appears to be quantitatively better at higher temperatures (723, 623 K) than at 523 K, which is quite close to the critical one ($T_c = 516$ K). We recall here that in the case of scMeOH[53] the agreement between simulation and experiment was found to be also quite good at 523 K. To explore the discrepancy between the NMR experiment and simulation observed at 523 K and the densities corresponding to the pressures in the range of 100−300 bar, it should be very useful to compare the simulated $\langle n_{HB} \rangle$ values with predictions from other experimental techniques. Such a comparison of our MD $\langle n_{HB} \rangle$ data with corresponding experimental results, especially with those from the IR and Raman[49,51] studies, is not feasible at the present time because the acquired experimental values n_{HB} for scEtOH have not been reported in that or in subsequent publications.

According to the results obtained for the H-bond statistics (see Table 4), scEtOH mainly forms one H-bond per molecule. In contrast to this result, the statistics for liquid EtOH show a quite different behavior. The most significant percentage (78.64%) of the molecules in the liquid appears to have two H-bonds. Also, our calculations provide a significant value of the percentage of monomers ($i = 0$), which is between 35.25 and 92.22% in the SC state and less than 2% in the liquid one. Note that the percentage of monomers in the sample is found to be considerably high in the low-density region and still significant for the fluid at the state points with densities about twice that of the critical one (A−C). Moreover, the percentage of molecules with two H-bonds ($i = 2$) obtained in the SC state is also significant. Finally, it is found that in the high-density region the percentage of f_3 still exists, while that of f_4 becomes negligible.

Therefore, it follows from our results that the intermolecular structure of scEtOH is basically formed by a significant number of monomer molecules while the rest of them are H-bonded mainly in dimers and trimers as well as in a markedly small number of tetramers. Additionally, the careful analysis[58] of our every 50 time steps stored MD configurations has shown that the chains with three and maximum of four H-bonded molecules observed are still linear in the high-density region (A−C) of the fluid studied. The complete results of this analysis as well as the dynamics of the H-bonded relatively small clusters in scEtOH will be presented elsewhere.

As mentioned above, to obtain a visual picture of the H-bonding phenomenon and possible molecular aggregates in the fluid, we have constructed some animations using the stored MD produced trajectories of the fluid. Note also that some snapshots of individual configurations were selected emphasizing the existence of some oligomers identified in the sample throughout the implementation of the H-bonding search procedure. Figures 10 and 11 show two representative configurations (snapshots) of the fluid from this MD study at 523 and 723 K, respectively. From these figures it can be seen that scEtOH molecules form aggregates, which are more apparent in Figure 10a corresponding to the fluid at high density (state B). The regions with monomers in the fluid are shown in Figure 10b, which has been constructed from Figure 10a by not displaying all the H-bonded molecules in the sample. It is also

TABLE 5: Estimation of the Average Percentage *f* of the Monomer and Free Molecules in the Sample of scEtOH at 523, 623, and 723 K and Densities Corresponding to the Pressures in the Range 20−300 Bar[a]

				$T = 523$ K			
ρ/g cm^{-3}	0.0216	0.13	0.464	0.523	0.566	0.602	liquid
monomer	90.78	70.35	41.91	37.57	35.48	35.25	1.21
free	95.00	83.00	63.35	60.31	58.33	57.89	11.25

$T = 623$ K			
ρ/g cm^{-3}	0.132	0.339	0.447
monomer	82.88	65.74	58.47
free	90.85	80.49	75.98

$T = 723$ K			
ρ/g cm^{-3}	0.090	0.207	0.312
monomer	92.22	83.67	76.59
free	95.97	91.37	87.34

[a] Results for the liquid at normal conditions are also shown.

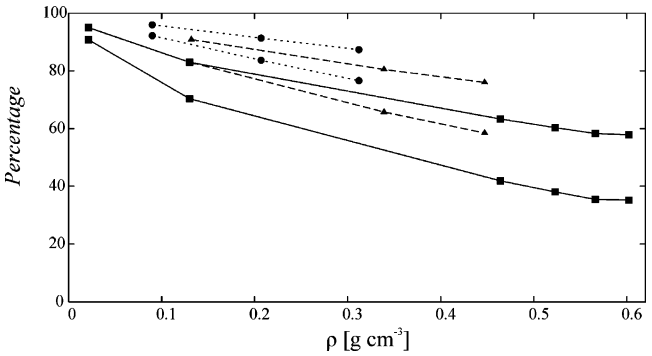

Figure 12. Percentage of monomers and free molecules obtained from this MD study of supercritical ethanol as a function of density and for three isotherms: (— 523 K), (- - - 623 K), (··· 723 K). In all isotherms, the upper curve corresponds to the percentage of free molecules.

apparent from this configuration the formation mainly of dimer and some linear trimers as well as very few tetramers are displayed in Figure 10c, where all the identified monomers in the system are not shown.

Another topic of interest here is the percentage of monomers and free scEtOH molecules, as investigated by IR and Raman vibrational spectroscopy[51] and by using the aforementioned search method in this MD study. The results obtained for the percentage of monomers and free OH groups from this study at different temperatures with density are reported in Table 5 and depicted in Figure 12. A careful examination of these results shows that at each temperature studied here the percentage of monomers and free OH groups is not negligible at high densities. Furthermore, at densities below the critical one (0.28 g cm^{-3}), a very strong increase in this percentage has been observed. As mentioned above, the analysis of the IR and Raman spectra of scEtOH at 523 K and densities in the range up to 0.6 g cm^{-3} by Besnard and co-workers has allowed these authors to evaluate the percentage of free OH groups shown in Figure 8 and Table 3 in ref 51. Concretely, from that table their percentage predictions of the free OH bonds from IR and Raman at $T =$ 523 K, $P = 6.0$ MPa, and $\rho = 0.13$ g cm^{-3} are 64 and 59.8, respectively. On the other hand, our MD result at the same state point (see Table 5) is 83%, a value higher than the experimental one. Note also that the percentage of the free OH bonds from this MD study (95%) is found to be in relatively good agreement with the result from that experimental work at $T = 523$ K and a very low density of 0.0216 g cm^{-3} (see Figure 8 in ref 51).

4. Conclusions

In this paper, a NVT molecular dynamics simulation study of SC and liquid EtOH has been carried out in order to explore the H-bonding structure of the fluid in a wide range of temperatures and pressures. For the SC fluid, the simulations were performed at three isotherms, namely, 523, 623, and 723 K and pressures ranging between 2 and 30 MPa, which led to densities in the range of 0.022−0.602 g cm^{-3}. The liquid was simulated at ambient conditions. Also, the fluid was studied at thermodynamic conditions for which thermodynamic and spectroscopic data are available in the literature. All molecules were modeled as semiflexible objects and bending interactions were used. The most interesting pdf's were calculated, and their temperature and pressure or density dependence were obtained and discussed. It is found that over the thermodynamic conditions investigated here, scEtOH remains highly structured. Examination of the site−site correlations of the SC fluid shows that the characteristic behavior of the first peaks in H−H, O−O, and H−O pdf's reveals that hydrogen bonds still exist in scEtOH.

More insights on the H-bonding structure of the fluid at each state point of interest were obtained on the basis of a well-defined geometric criterion. Using a standard procedure, we analyzed very long molecular trajectories to explore the H-bonds in the fluid and to evaluate reliable H-bond statistics. This methodology allowed us to estimate the average total number of H-bonds per molecule, n_{HB}, and the percentage f_i of molecules involved in i ($i = 0, 1, 2, 3, ...$) H-bonds. Furthermore, we computed the percentage of free OH bonds and that of monomers in the fluid. Our analysis indicates that the percentage of monomers is less 2% in the liquid state and between 34 and 92% in the SC one. In addition, in scEtOH the free OH bonds are present with a percentage increasing from a value of 58% ($\rho = 0.602$ g cm^{-3}) to a value of 95% ($\rho = 0.02$ g cm^{-3}) by decreasing the density. The degree of aggregation (average number of H-bonds per molecule) was compared with previous results from NMR chemical shift studies.[40] It is found that the agreement between experiment and simulation appears to be quantitatively better at higher temperatures (723, 623 K) than at $T = 523$ K, a temperature which is close to the critical one ($T_c = 516$ K). Also, the estimated monomer and free OH groups in the fluid were compared with results from IR and Raman vibrational spectroscopy of scEtOH at $T = 523$ K.[51] While the simulated percentage of monomers and free OH bonds agrees very well with experiments in the low-density region below the critical one, it appears that these results are in discrepancy in the high-density region. At this point, we have to mention that Soetens et al.,[73] from the Bordeaux group, performed also a H-bond analysis of scEtOH based on MD simulation of the fluid at 523 K in order to support their spectroscopic predictions (results have not been reported yet). As mentioned by these researchers, in the case of scEtOH discrepancies between MD and spectroscopic analysis were also observed and this point is still unclear. On the other hand, Andanson et al.[74] in a most recent paper reported results on H-bonding in SC *tert*-butyl alcohol assessed by vibrational spectroscopies and MD simulations at $T = 523$ K and densities in the range 0.05−0.4 g cm^{-3}. They pointed out that in SC fluid the free OH bonds are dominant with a percentage from 65 to 85% as the system density decreases. Also, the percentage of monomers is found to be between 45 and 74% at these densities. Generally, they found very consistent results between experiment and the MD simulation. Note that this picture exhibits similarities with our

MD results for scEtOH concerning the percentage of the free OH bonds and monomers in these fluids.

Generally, the main conclusion that may be drawn is that the intermolecular structure of scEtOH is basically formed by a significant number of monomer molecules while the rest of them are H-bonded mainly in dimers and linear chain trimers as well as in a markedly small number of linear tetramers.

In the case of dynamic properties of the SC fluid, the present attempt focuses also on the reorientational dynamics of the bond unit vectors O−H, C−O, and the permanent dipole moment of the molecules, as well as the total dipole moment of the sample. The corresponding Legendre tcf's were discussed in connection to the "hydrogen bonding" in the fluid and experiment. Specifically, the behavior of the O−H dynamics exhibits the well-known associative behavior of the EtOH molecules in the SC fluid. The MD τ_2^{H-O} reorientational times for $T = 523$ K and state points A−C (0.464−0.602 g cm^{-3}) are in the range 0.23−0.29 ps, which are in quite good agreement with those from NMR in the high-density region. Moreover, three supplementary MD runs at 523 K and densities 0.0216, 0.130, and 0.523 g cm^{-3} provided τ_2^{H-O} reorientational times of 0.10, 0.22, and 0.24 ps, respectively, which compared to the experimental ones at the same densities were found to be in excellent agreement.

Finally, we have also calculated the dielectric properties of the system such as the static dielectric constant $\epsilon(0)$ and the Debye relaxation time τ_D. The calculation of the aforementioned properties was based upon a very long trajectory of the simulated scEtOH at 523 K and 100, 200, and 300 bar. The MD results obtained for the static dielectric constant $\epsilon(0) = 4.2$ and the Debye relaxation time $\tau_D = 1.04$ ps at 523 K and 200 bar of scEtOH have been compared with available experimental data reported in a recent dielectric relaxation study by Hiejima and Yao. The previous study for temperatures and pressures in the ranges 513−533 K and 14.8−22.3 MPa, respectively, provides experimental values for $\epsilon(0)$ which are between 3.8 and 4.2, and τ_D times in the range 4.6−4.1 ps. In summary, our calculated dielectric properties $\epsilon(0)$ and τ_D led us to conclude that the static dielectric constant shows a quantitative agreement with corresponding experimental data, while the Debye relaxation time from the simulation is somewhat shorter compared with the experimental one.

From the MD study presented in this paper, we may conclude that scEtOH molecules form small linear oligomers (dimers, trimers, and tetramers) with an average of less than one H-bond per molecule.

Acknowledgment. We are grateful to Prof. M. Besnard and Dr. J.-C. Soetens (UMR CNRS-Université Bordeaux 1, France) for sending us the manuscript of their recently accepted work concerning investigation of hydrogen bonding in supercritical *tert*-butyl alcohol prior to publication. J.S. acknowledges the use of the supercomputing facilities provided by the Research Oriented Computing Center John von Neumann-Institute for Computing NIC-ZAM, Jülich, Germany.

References and Notes

(1) Pimentel, G. C.; Mcclellan, A. L. *The Hydrogen Bond*; Reinhold Publishing Corp.: New York, 1960.

(2) Pauling, L. *The Nature of the Chemical bond and the Structure of Molecules and Crystals: An Introduction to Modern Structural Chemistry*; Cornell University Press: Ithaca, NY, 1960.

(3) Schuster, P.; Zundel, G.; Sandorfy, C. *The Hydrogen Bond*; North-Holland Publishing Co.: Amsterdam, 1976; Vol. 13.

(4) Weber, A., Ed. *Structure and Dynamics of Weakly Bound Molecular Complexes*; NATO ASI Series C: Mathematical and Physical Sciences; Reidel Publishing Co.: Tokyo, 1987; Vol. 212D.

(5) Dore, J., Texeira, J., Eds. *Hydrogen Bonded Liquids*; NATO ASI Series C: Mathematical and Physical Sciences; Kluwer Academic Publishers: Boston, MA, 1991; Vol. 329.

(6) Ludwig, R.; Gill, D. S.; Zeidler, M. D. *Z. Naturforsch*. **1992**, *47a*, 857.

(7) Bellisent-Funel, M. C., Dore, J., Eds. *Hydrogen Bond Networks*; NATO ASI Series C, Mathematical and Physical Sciences; Kluwer Academic Publishers: Boston, MA, 1994; Vol. 435.

(8) Buckingham, A. D. In *Theoretical treatments of hydrogen bonding*; Hadzi, D., Ed.; Wiley: New York, 1997; p 1.

(9) Fayer, M. D., Ed. *Ultrafast infrared and Raman spectroscopy*; Marcel Dekker: New York, 2001.

(10) Elsaesser, T., Bakker, H. J., Eds. *Ultrafast hydrogen bonding dynamics and proton-transfer processes in the condensed phase*; Kluwer: Dordrecht,The Netherlands, 2002.

(11) Bratos, S.; Gale, G.; Gallot, G.; Hache, F.; Lascoux, N.; Leicknam, J.-Cl. *Phys. Rev. E* **2000**, *61*, 5211.

(12) Fecko, C. J.; Loparo, J. J.; Roberts, S. T.; Tokmakoff, A. *J. Chem. Phys.* **2005**, *122*, 054506.

(13) Nibbering, E. T. J.; Elsaesser, T. *Chem. Rev.* **2004**, *104*, 1887.

(14) Bratos, S.; Leicknam, J.-Cl.; Mirloup, F.; Vuilleumier, G.; Gallot, M. In *Novel Approaches to the Structure and Dynamics of Liquids: Experiments, Theories and Simulation*; Samios, J., Durov, A., VI, Eds.; NATO ASI Science Series II, Mathematics, Physics and Chemistry; Kluwer Academic Publishers: Dordrecht, The Netherlands, 2004; Vol. 133, p 111.

(15) Jorgensen, W. L. *J. Phys. Chem*. **1986**, *90*, 1276.

(16) Haughney, M.; Ferrario, M.; McDonald, I. R. *J. Phys. Chem*. **1987**, *91*, 4939.

(17) Mountain, R. *J. Chem. Phys.* **1989**, *90*, 1866.

(18) Ferrario, M.; Haughney, M.; McDonald, I. R.; Klein, M. L. *J. Chem. Phys.* **1990**, *93*, 5156.

(19) Kalinichev, A. *Z. Naturforsch.* **1991**, *46A*, 433.

(20) Cochran, H.; Cummings, P.; Karaborni, S. *Fluid Phase Equilib.* **1992**, *71*, 1.

(21) Chialvo, A. A.; Cummings, P. T. *J. Chem. Phys*. **1994**, *101*, 4466.

(22) Kalinichev, A.; Bass, *J. Chem. Phys. Lett*. **1994**, *231*, 301.

(23) Cummings, P.; Chialvo, A.; Cochran, H. *Chem. Eng. Sci*. **1994**, *49*, 2735.

(24) Luzar, A.; Chandler, D. *J. Chem. Phys*. **1990**, *98*, 8160.

(25) Guardia, E.; Marti, J.; Padro, J. A.; Saiz, L.; Komolkin, A. V. *J. Mol. Liq.* **2002**, *96−97*, 3.

(26) Palinkas, G.; Bako, I.; Heinziker, K.; Bopp, P. *Mol. Phys*. **1991**, *73*, 897.

(27) Mancera, R. L.; Chalaris, M.; Refson, K.; Samios, J. *Phys. Chem. Chem. Phys*. **2004**, *6*, 94.

(28) Mancera, R. L.; Chalaris, M.; Samios, J. *J. Mol. Liq*. **2004**, *110*, 147.

(29) Roney, A. B.; Space, B.; Castner, E. W.; Napoleon, R. L.; Moore, P. B. *J. Phys. Chem. B* **2004**, *108*, 7389.

(30) Special issue dedicated to supercritical fluids. *Chem. Rev*. **1999**, *99*, 353.

(31) Johnston, K. P., Kim, S., Penninger, J. M. L., Eds. *Supercritical fluid Science and Technology*; American Chemical Society: Washington, DC, 1998; Chapter 5 and refs therein.

(32) Tucker, S. *Chem. Rev*. **1999**, *9*, 391.

(33) Shaw, R. W.; Brill, B.; Clifford, A.; Eckert, A.; Frank, E. U. *Chem. Eng. News* **1991**, *69*, 26.

(34) Mizan, T. I.; Savage, P. E.; Ziff, R. M. *J. Phys. Chem*. **1996**, *100*, 403.

(35) Tassaing, T.; Bellisent-Funel, M. C.; Guillot, B.; Guissani, Y. *Eur. Lett*. **1998**, *42*, 265.

(36) Guillot, B.; Guissani, Y. *Fluid Phase Equilib*. **1998**, *150*, 19.

(37) Guillot, B. *J. Mol. Liq*. **2002**, *101*, 219.

(38) Lu, J.; Boughner, E. C.; Liotta, C. L.; Eckert, C. A. *Fluid Phase Equilib*. **2002**, *198*, 37.

(39) Dobbs, J. M.; Wong, J. M.; Lahiere, R. J.; Johnston, K. P. *Ind. Eng. Chem. Res*. **1987**, *26*, 56.

(40) Hoffmann, M. M.; Conradi, M. S. *J. Phys. Chem. B* **1998**, *102*, 263.

(41) Bai, S.; Yorker, C. R. *J. Phys. Chem. A* **1998**, *102*, 8641.

(42) Asahi, N.; Nakamura, Y. *J. Chem. Phys*. **1998**, *109*, 9879.

(43) Tsukahara, T.; Harada, M.; Ikeda, Y.; Tomiyasu, H. *Chem. Lett*. **2000**, *4*, 420.

(44) Yamaguchi, T.; Matubayasi, N.; Nakahara, M. *J. Phys. Chem. A* **2004**, *108*, 1319.

(45) Yamaguchi, T.; Benmore, C. J.; Soper, A. K. *J. Chem. Phys*. **2000**, *112*, 8976.

(46) Ebukuro, T.; Takami, A.; Oshima, Y.; Koda, S. S. *Supercrit. Fluids* **1999**, *15*, 73.

(47) Lalanne, P.; Tassaing, T.; Danten, Y.; Besnard, M. *J. Mol. Liq*. **2002**, *98*−*99*, 201.

(48) Bulgarevich, D. S.; Otake, K.; Sako, T.; Sugeta, T.; Takebayashi, Y.; Kamizawa, C.; Shintani, D.; Negishi, A.; Tsurumi, C. *J. Chem. Phys*. **2002**, *116*, 1995.

(49) Barlow, S. J.; Bonclarenko, G. V.; Gorbaty, Y. E.; Yamaguchi, T.; Poliako, M. *J. Phys. Chem. A* **2002**, *106*, 10452.

(50) Hiejima, Y.; Yao, M. *J. Chem. Phys*. **2003**, *119*, 7931.

(51) Lalanne, P.; Andanson, J. M.; Soetens, J.-C.; Tassaing, T.; Danten, Y.; Besnard, M. *J. Phys. Chem. A* **2004**, *108*, 3902.

(52) Gupta, R. B.; Panayiotou, C. G.; Sanchez, I. C.; Johnston, K. P. *AIChE J.* **1992**, *38*, 1243.

(53) Chalaris, M.; Samios, J. *J. Phys. Chem B* **1999**, *103*, 1161.

(54) Chalaris, M.; Samios, J. *Pure Appl. Chem.* **2004**, *76*, 203.

(55) Honma, T.; Liew, C. C.; Inomata, H.; Arai, K. J. *Phys. Chem. A* **2003**, *107*, 3960.

(56) Chatzis, G.; Samios, J. *Chem. Phys. Lett.* **2003**, *374*, 187.

(57) Padro, J. A.; Saiz, L.; Guardia, E. *J. Mol. Struct*. **1997**, *416*, 243.

(58) Saiz, L.; Padro, J. A.; Guardia, E. *J. Phys. Chem. B* **1997**, *101*, 78.

(59) Paolantoni, M.; Ladanyi, B. M. *J. Chem. Phys*. **2002**, *117*. 3856.

(60) The supercritical ethanol density data were available from the authors in ref 40.

(61) Allen, M. P.; Tildesley, D. J. *Computer Simulation of Liquids*; Oxford University Press: Oxford, U.K., 1987.

(62) *CRC Handbook of Chemistry and Physics*, 74th ed.; New York, 1994.

(63) Berendsen, H. J. C.; Postma, J. P. M.; van Gusteren, W. F.; DiNola, A.; Haak, J. R. *J. Chem. Phys*. **1984**, *81*, 3684.

(64) Ryckaert, J. P. *Mol. Phys*. **1985**, *55*, 549.

(65) Smith, B. D.; Srivastava, R. *Thermodynamic Data for Pure Compounds*; Elsevier: Amsterdam, 1896.

(66) Jorgensen, W. L.; Maxwell, D. S.; Tirado-Rives, J. *J. Am. Chem. Soc.* **1999**, *118*, 11236.

(67) Hubbard, P. S. *Phys. Rev*. **1963**, *131*, 1155.

(68) Boettcher, C. J. F. *Theory of Electric Polarisation*; Elsevier: Amsterdam, 1973.

(69) De Leeuw, S. W.; Perram, J. W.; Smith, E. R. *Annu. Rev. Phys. Chem*. **1986**, *37*, 245.

(70) Kurnikova, M. G.; Balabai, N.; Waldeck, D. H. Coalson, R. D. *J. Am. Chem. Soc*. **1998**, *120*, 6121.

(71) Chalaris, M.; Samios J. *J. Chem. Phys*. **2000**, *112*, 8581.

(72) Saiz, L.; Guardia, E.; Padro, J.-A. *J. Chem. Phys*. **2000**, *113*, 2814.

(73) Soetens, J.-C. Private communication.

(74) Andanson, J.-M.; Soetens, J.-C.; Tassaing, T.; Besnard, M. *J. Chem. Phys. B* **2005**, *122*, 174512.